J2.3 Large-Eddy Simulation of the Roughness Sublayer within and above Forest Canopies and Its Transition to the Outer Regions of the Atmospheric Boundary Layers

Hong-Bing Su [1*] and Edward G. Patton[2]
[1] *East Carolina University, Greenville, NC, USA*
[2] *National Center for Atmospheric Research, Boulder, CO, USA*

1. INTRODUCTION

Most previous large-eddy simulations (LES) of airflow within and above forest and other plant canopies (Shaw and Schumann 1992, Kanda and Hino 1994, Dwyer et al. 1997, Shen and Leclerc 1997, Su et al. 1998, 2000, Patton et al. 2001, Albertson et al. 2001, Shaw and Patton 2003, Fitzmaurice et al. 2004, Watanabe 2004) are limited in both horizontal and vertical domain sizes relative to canopy heights. On the other hand, the roughness sublayer is not explicitly resolved in most LES of the atmospheric boundary layer (ABL) and its effect is simply represented by a prescribed roughness length (z_0). An exception is the work by Patton et al. (2003) where a nested-grid LES is used to study the influence of a forest canopy on top-down and bottom-up diffusions in a convective boundary layer. There is still a need to investigate how the ABL depth and stability and canopy morphology may influence the depth of the roughness sublayer, the characteristics of coherent structures in the roughness sublayer and their interactions with turbulence in the outer regions of the ABL.

With increasing computer power, high-resolution LES with realistic ABL depths and sufficient spatial resolution for the roughness sublayer become feasible. Here we present some preliminary results from an LES of an Ekman boundary layer (a pure neutral case).

2. METHOD

The LES formulation used here was originally developed by Moeng (1984) with subsequent refinements (Moeng and Wyngaard 1988). It was modified to simulate airflow within and above a forest canopy (Su et al. 1998) and the original code is adapted to run on a SunBlade2000 workstation for the case presented here.

A domain of $480 \times 480 \times 1920\ m^3$ is resolved by 120 x 120 x 480 equally spaced grids in the east (x), north (y) and vertical (z) directions. We recognize that the horizontal domain is still limited for a shear-driven ABL. The flow is driven by a geostrophic wind (U_g, V_g) = (10, 0) m s^{-1} with the Coriolis parameter (f) set to $1\text{x}10^{-4}\ s^{-1}$. The model forest is the same as that in Su et al. (1998, 2000) with a height (h_c) of 20 m and leaf area index (LAI) of 2. The drag coefficient (C_d) is 0.15 as in previous studies.

The simulation is integrated for about 17 h with 70 samples in the last 1.7 h taken for the results shown here. With a friction velocity (u_*) of 0.54 m s^{-1} and a boundary layer depth (z_i) of 480 m, the large-eddy turnover time would be about 0.25 h.

* *Corresponding author: Department of Geography, East Carolina University, Greenville, NC 27858-4353. Email: suh@ecu.edu.*

3. RESULTS AND DISCUSSIONS

3.1. Vertical Profiles of Single-Point Statistics

The height above ground (z) may be normalized in several ways. One is to use the canopy height (h_c) if the focus is on the roughness sublayer. The second is the boundary layer depth (z_i) as for shear-driven ABL with a capping inversion (Moeng and Sullivan 1994, Lin et al. 1996, 1997). The third is to use u_*f for an Ekman boundary layer (Andrén and Moeng 1993) in which the boundary layer depth may be defined as the height where momentum flux is reduced to a certain percentage of its surface value. Here we define z_i = 480 m = 24h_c which has a similar value to those in Moeng and Sullivan (1994) and Lin et al. (1996, 1997) and that it is the height at which an inflection in mean wind speed is located below the maximum wind speed.

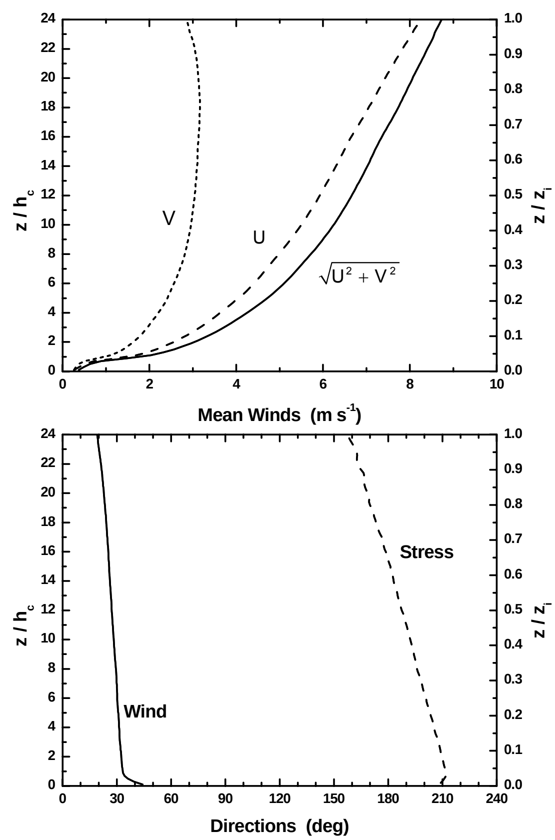

Fig. 1. Vertical profiles of mean wind speeds (U, V) in the x and y directions and of directions of mean wind and Reynolds stress.

As expected, vertical gradients of mean wind direction are the greatest within the forest (Fig. 1), whereas above canopy, they are similar to those shown in Moeng and

Sullivan (1994) and Lin et al. (1996). This vertical wind directional shear is absent in most previous LES of airflow within plant canopies as the Coriolis force was not included. In contrast, the directions of Reynolds stress are fairly constant in the canopy.

The values of normalized momentum fluxes $\overline{uw}/u_*^2$ and $\overline{vw}/u_*^2$ (Fig. 2) at the canopy top have better agreement with the surface values shown in Moeng and Sullivan (1994) than those in Andrén and Moeng (1993). The height at which $\overline{vw}/u_*^2$ becomes negative is similar to that in Moeng and Sullivan (1994), but the near-linear decrease of $\overline{uw}/u_*^2$ with height is less rapid.

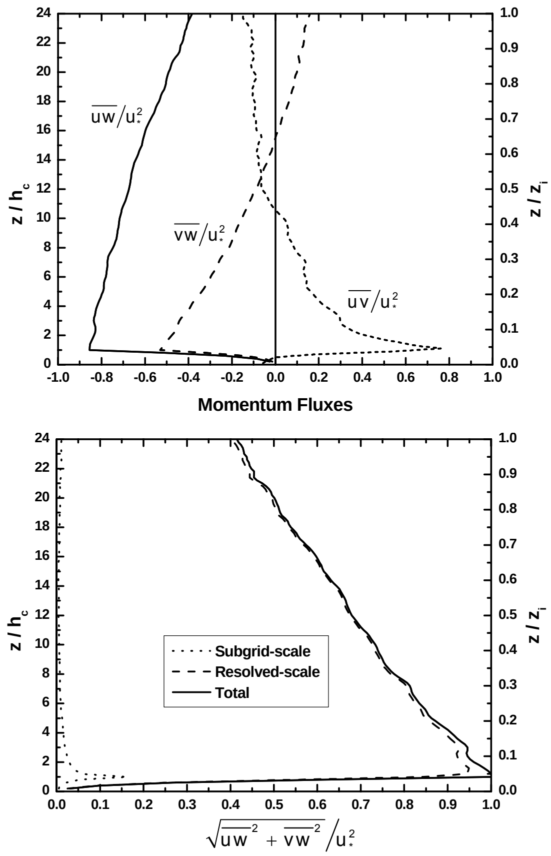

Fig. 2 Vertical profiles of normalized momentum fluxes. In the upper panel, both resolved-scale and subgrid-scale contributions are included.

Obviously, the magnitudes of velocity variances could differ in different coordinate for anisotropic flow. This needs to be considered when comparing LES results with field observations in the surface layer where a common practice is to define the mean wind direction at the measurement height as the streamwise direction. In this coordinate (denoted by the subscript m) and for the resolved-scale flow field, $\overline{u_m^2}/u_*^2$ and $\overline{v_m^2}/u_*^2$ are greater and smaller than their respective values $\overline{u^2}/u_*^2$ and $\overline{v^2}/u_*^2$ in the x-y coordinate between $1h_c$ and $4h_c$ (upper panel of Fig. 3). The opposite is true above $6h_c$.

Maximum velocity variances are not located right at the canopy top but at some levels from just above the canopy top to $2h_c$. The characteristics of these velocity variances profiles in the surface layer are in better agreement with those in Lin et al. (1997) where the vertical resolution is much higher than those in Moeng and Sullivan (1994) and in Andrén and Moeng (1993). For example, the maximum $\overline{u_m^2}/u_*^2$ (lower panel of Fig. 3) is about 4.14, closer to 4.2-4.4 in Lin et al. (1997) than 5.3 in Moeng and Sullivan (1994) and 5.9 in Andrén and Moeng (1993). Lin et al. (1997) also show that this value is smaller for a rougher surface. As discussed below, the roughness length in our case (z_0 = 3 m) is greater than that of the roughest surface (z_0 = 0.83 m) in Lin et al. (1997). It is also noted that the subgrid-scale kinetic energy (e) increases with height above z = $12h_c$.

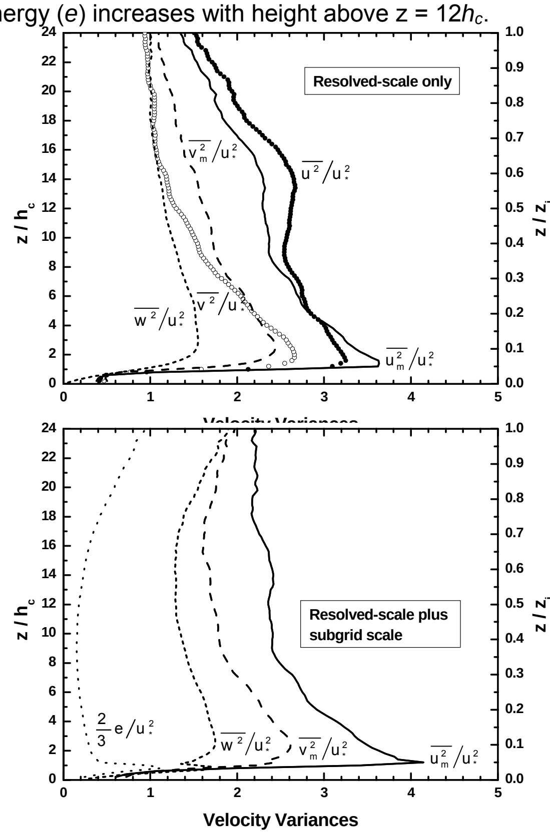

Fig. 3 Vertical profiles of normalized velocity variances. Curves are calculated with the mean wind direction as the streamwise direction at each height. The symbols in the upper panel are calculated in the *x* and *y* directions.

The vertical profile of normalized standard deviation of the pressure perturbations $\overline{p^2}^{1/2}/\rho u_*^2$ (Fig. 4) also agrees better with that in Lin et al. (1997) than that in Su et al. (1998). This could be due to the much smaller domain in Su et al. (1998) and that pressure perturbation at a given location is influenced by the entire flow field near or far albeit with different weight. The maximum $\overline{p^2}^{1/2}/\rho u_*^2$ is located at z = $1.5h_c$ and has a greater value than that in Lin et al. (1997) who also showed that this maximum value increases with surface roughness length.

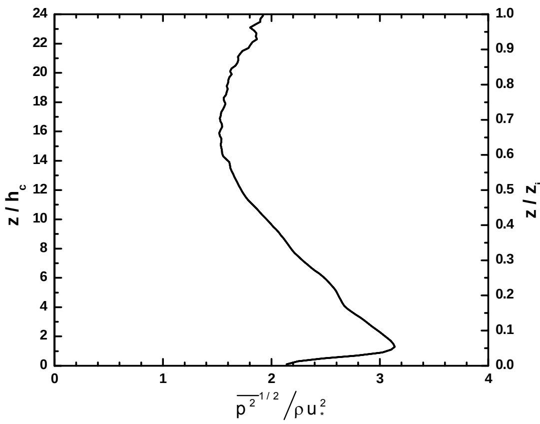

Fig. 4 Profile of standard deviation of fluctuating pressure.

In the x-y coordinate, all correlation coefficients ($\gamma_{uw} = \overline{uw}\Big/\left[\overline{u^2}\,\overline{w^2}\right]^{1/2}$, γ_{vw}, γ_{uv}) peak near the canopy top. This is only the case for $\gamma_{u_m w}$ in the coordinate with the streamwise direction in the mean wind direction at each height, and the peak value increases to 0.6, and is relatively constant (~0.43) between 2.5h_c and 8h_c (Fig. 5).

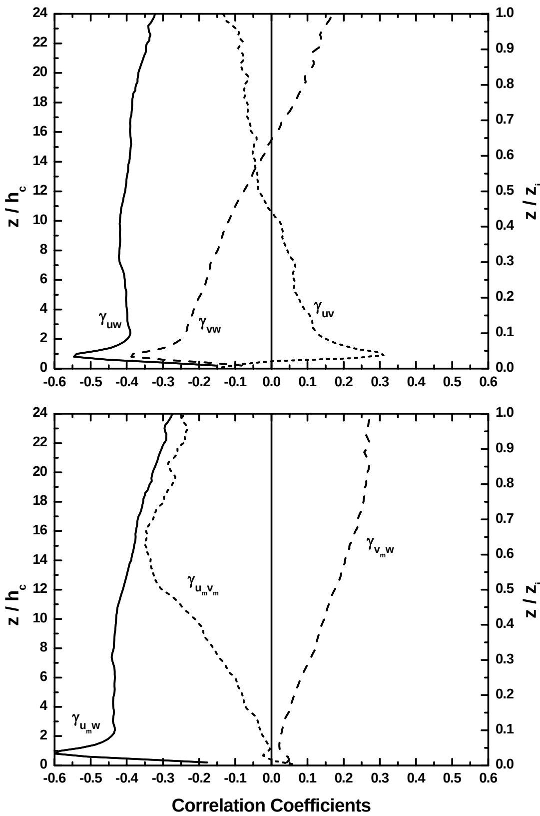

Fig. 5 Profiles of correlation coefficients between velocity components. Upper panel: x-y coordinate. Lower panel: mean wind direction coordinate.

Velocity skewness ($\overline{u_i^3}\Big/\overline{u_i^2}^{3/2}$) is also much greater (a measure of intermittency) from the ground to 2h_c and changes sign at about 2h_c (Fig. 6).

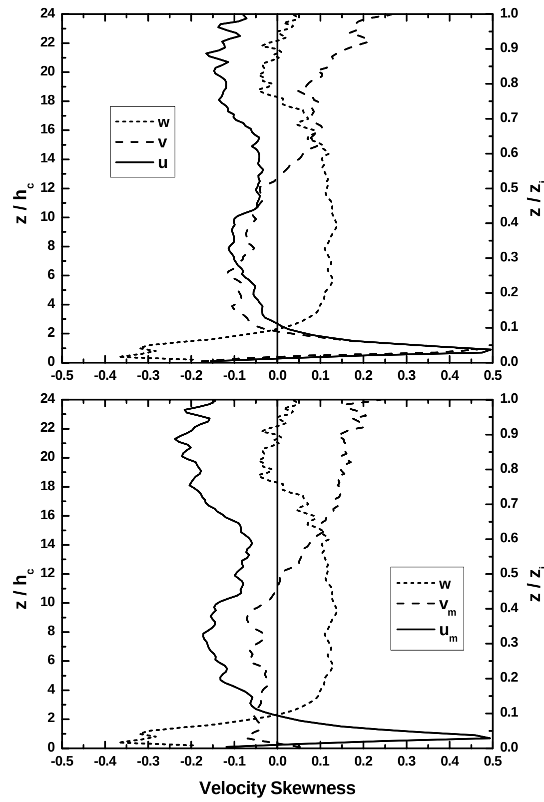

Fig. 6 Profiles of velocity skewness. Upper panel: x-y coordinate. Lower panel: mean wind direction coordinate.

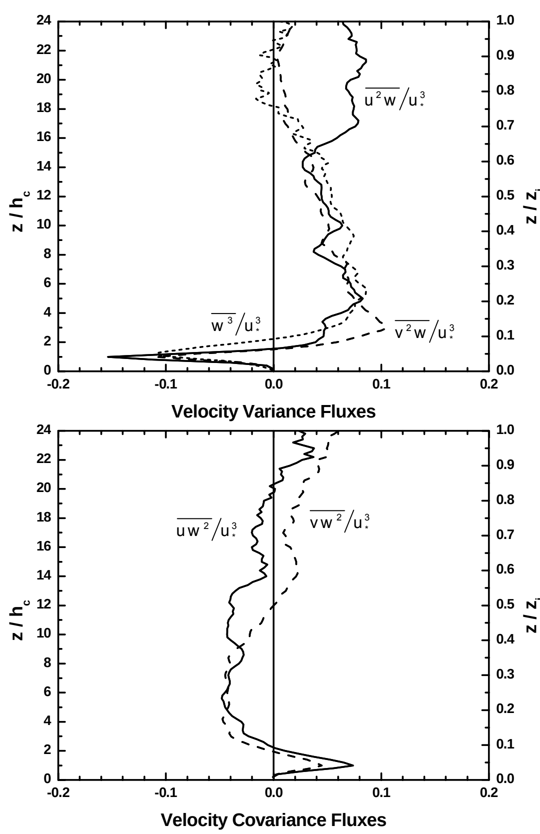

Fig. 7 Profiles of velocity variance and covariance fluxes.

The vertical profiles of the velocity variance and covariance fluxes suggest that turbulent transports are source terms in the budgets of the velocity variances and covariances in a layer from near the canopy top to about 3-4h_c (Fig. 7). The opposite is true within the canopy and above 4h_c.

3.2. The Logarithmic Wind Profile

To estimate the roughness length (z_0) with the LES output, we include the zero-plane-displacement height (d) in the logarithmic wind profile. We estimate d = 14 m = 0.7h_c for the model forest as the mean level of momentum absorption (Su et al. 1998). It is clear that $\ln(z-d)-\kappa U/u_*$ is relatively constant (~1.1 which yields z_0 = 3 m = 0.15h_c) in a layer between 2h_c and 4h_c, whereas $\ln(z)-kU/u_*$ increases continuously with height (Fig. 8). Here $\kappa = 0.4$ is the von Kármán constant. Consequently, the simulated mean wind profile matches the logarithmic wind profile quite well in the same layer.

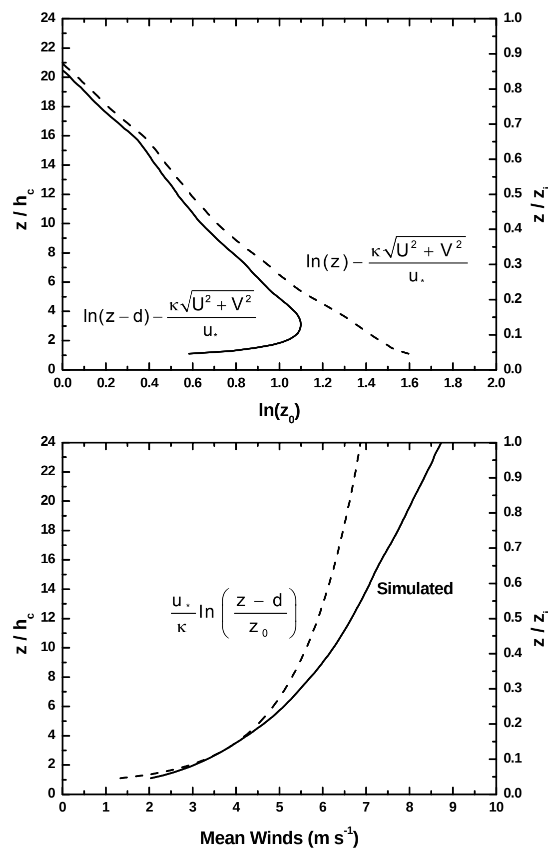

Fig. 8 Estimate of roughness length (upper panel) and the mean wind profiles (lower panel).

3.3. Eddy-Diffusivity

We may estimate the eddy-diffusivity for momentum as $K_M = u_*^2 \Big/ \sqrt{(\partial U/\partial z)^2 + (\partial V/\partial z)^2}$ using the LES output. Again, the surface layer parameterization $K_M = \kappa u_*(z-d)$ provides relatively good estimate only in a very thin layer between 2.5h_c and 3h_c (Fig. 9). The enhancement of eddy-diffusivity between the canopy top and 2.5h_c agrees with previous studies.

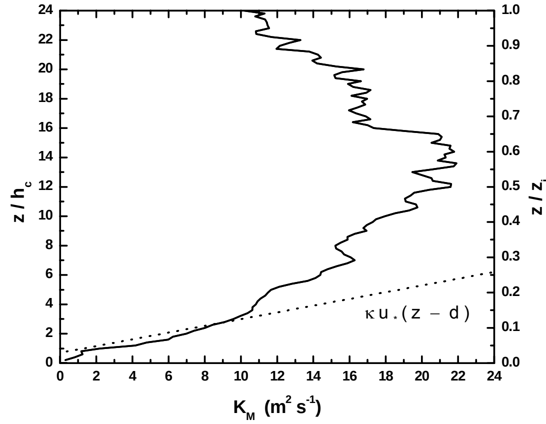

Fig. 9 Profile of eddy-diffusivity for momentum.

3.4. Pressure Transport

Pressure transport is an important term in the budget of turbulent kinetic energy in the roughness sublayer within and above a forest canopy (Dwyer et al. 1997) and in the surface layer (Moeng and Sullivan 1994). For neutrally stratified ABL, the pressure flux term has been parameterized as $\overline{wp}/\rho = -0.2\overline{(u^2+v^2+w^2)w}$ (Zeman 1981). Our results show that this parameterization fails in the roughness sublayer (from the ground up to about 2h_c) and above 10h_c (Fig. 10). It works relatively well between 2h_c and 8h_c except that the proportional coefficient is not constant (0.2) with height but decreases from 0.74 at 2h_c to 0.16 at 8h_c.

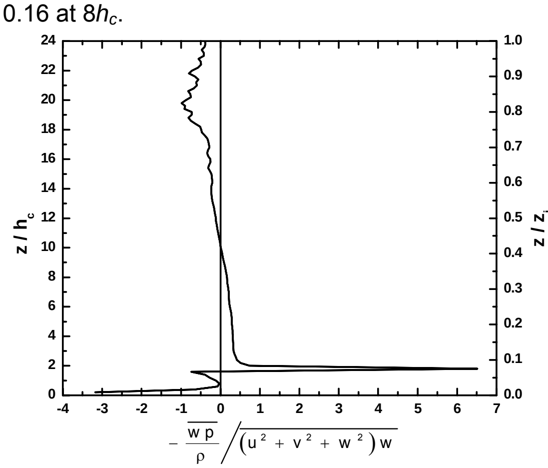

Fig. 10 Profile of the ratio between pressure flux and turbulent velocity variance flux.

3.5. Two-Point Auto-Correlations

The two-point auto-correlation for a flow variable α defined as $R_{\alpha\alpha}(r_x, r_y, r_z) = \overline{\alpha(x,y,z)\alpha(x+r_x, y+r_y, z+r_z)} \big/ \overline{\alpha^2}$ is useful to examine the spatial extent of coherent structures and to calculate spatial integral length scales. Here r_x, r_y, r_z are spatial separations in x, y, z directions.

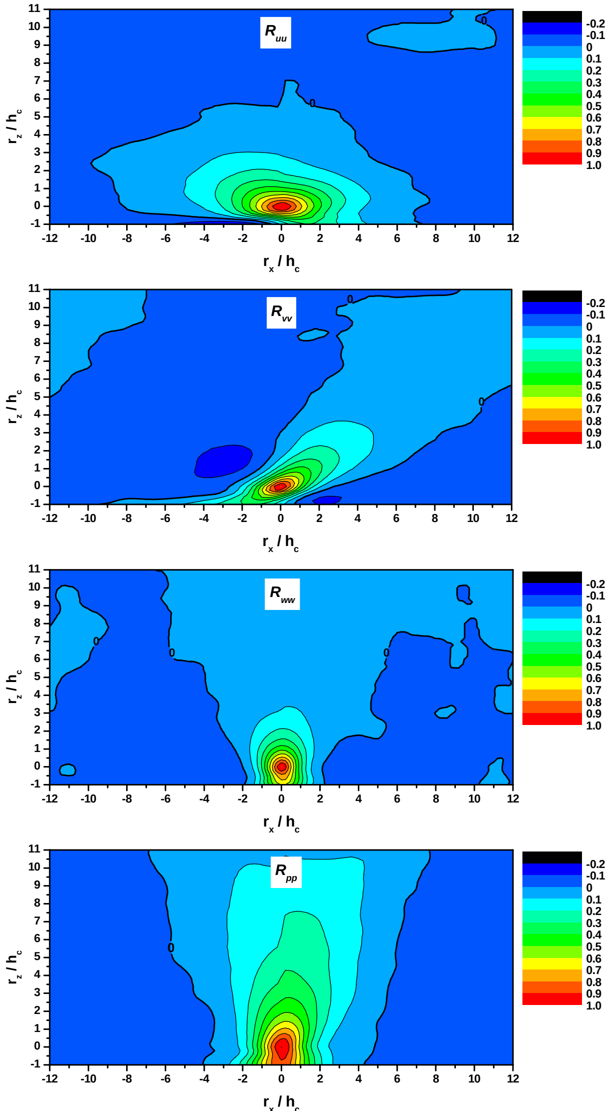

Fig. 11 Two-point auto-correlations with separations in the x and z directions ($r_y = 0$) and the reference near the canopy top.

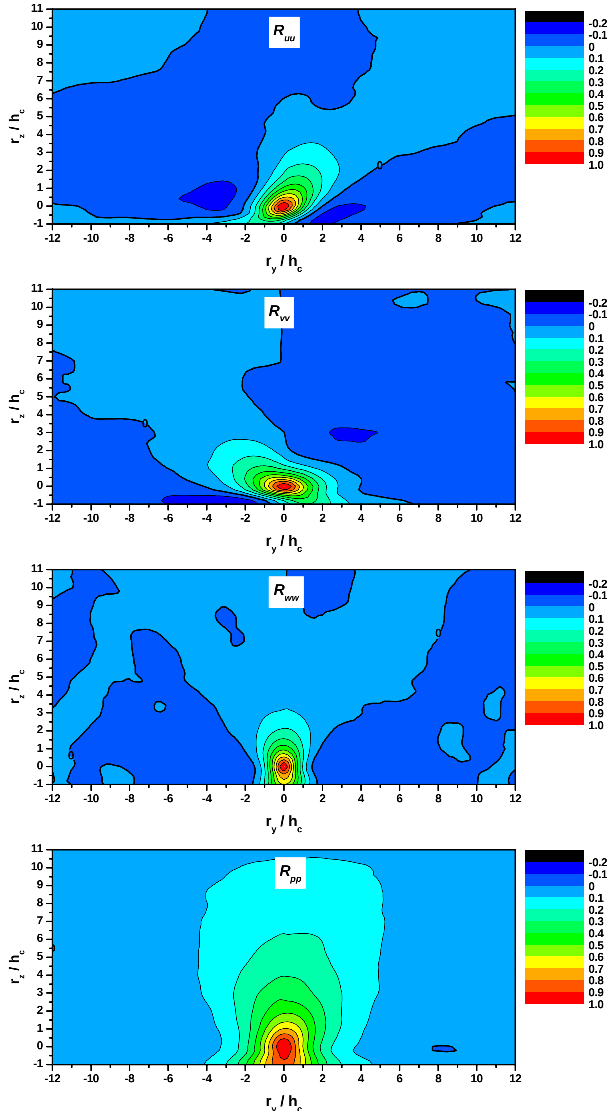

Fig. 12 Two-point auto-correlations with separations in the y and z directions ($r_x = 0$) and the reference near the canopy top.

Two-point auto-correlations with separations in the x and z directions (Fig. 11) and in the y and z directions (Fig. 12) with the reference at the canopy height illustrate similar features as those shown in Su et al. (2000). However, due to vertical mean wind directional shear in the present simulation, R_{uu} in the x-z plane resembles R_{vv} in the y-z plane, and R_{vv} in the x-z plane shows similar characteristics as R_{uu} in the y-z plane. The vertical extent (using 0.1 or 0.2 contour level as an indicator) is not substantially different from those shown in earlier LES of canopy airflow with much smaller vertical domain sizes (Su et al. 2000). The horizontal extent however, appears to be greater in the present results. This may be better seen from auto-correlations with separations in the x and y directions near the canopy top (Fig. 13). It is shown that R_{ww} and R_{pp} are elongated (aspect ratio ~ 2:1 using the 0.1 contour line) in the streamwise (along mean wind) and spanwise (crosswind) directions respectively.

As for the single-point statistics, two-point correlations for the horizontal velocities would differ in different coordinates. In the x-y coordinate, both R_{uu} and R_{vv} are also elongated in directions to the right and left of the mean wind direction respectively (Fig. 13). Similar to Lin et al. (1996, 1997), $R_{u'u'}$ and $R_{v'v'}$ (Fig. 14) are auto-correlations for the streamwise (u') and spanwise (v') velocities in a coordinate with the streamwise direction defined as the mean Reynolds direction at a given height. In this coordinate, $R_{u'u'}$ remains elongated whereas $R_{v'v'}$ is more isotropic in horizontal directions.

The distance between the center of the two negative side lobes in $R_{u'u'}$ may be a measure of the spacing between low speed streaks which increases linearly with height in the surface layer when scaled with the boundary layer depth z_i (Lin et al. 1997). In the roughness sublayer, this distance is ~8h_c at z = 1.1h_c and ~12h_c at z = 1.9h_c.

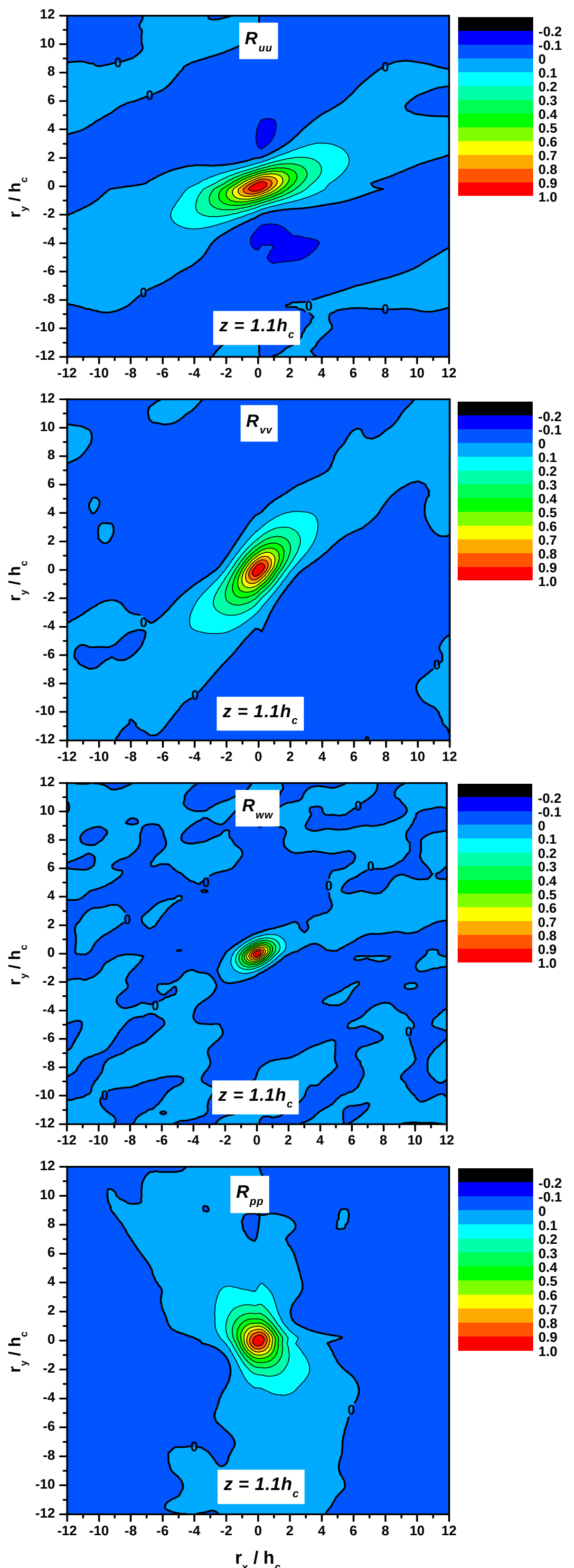

Fig. 13 Two-point auto-correlations with separations in the x and y directions ($r_z = 0$) and the reference near the canopy top.

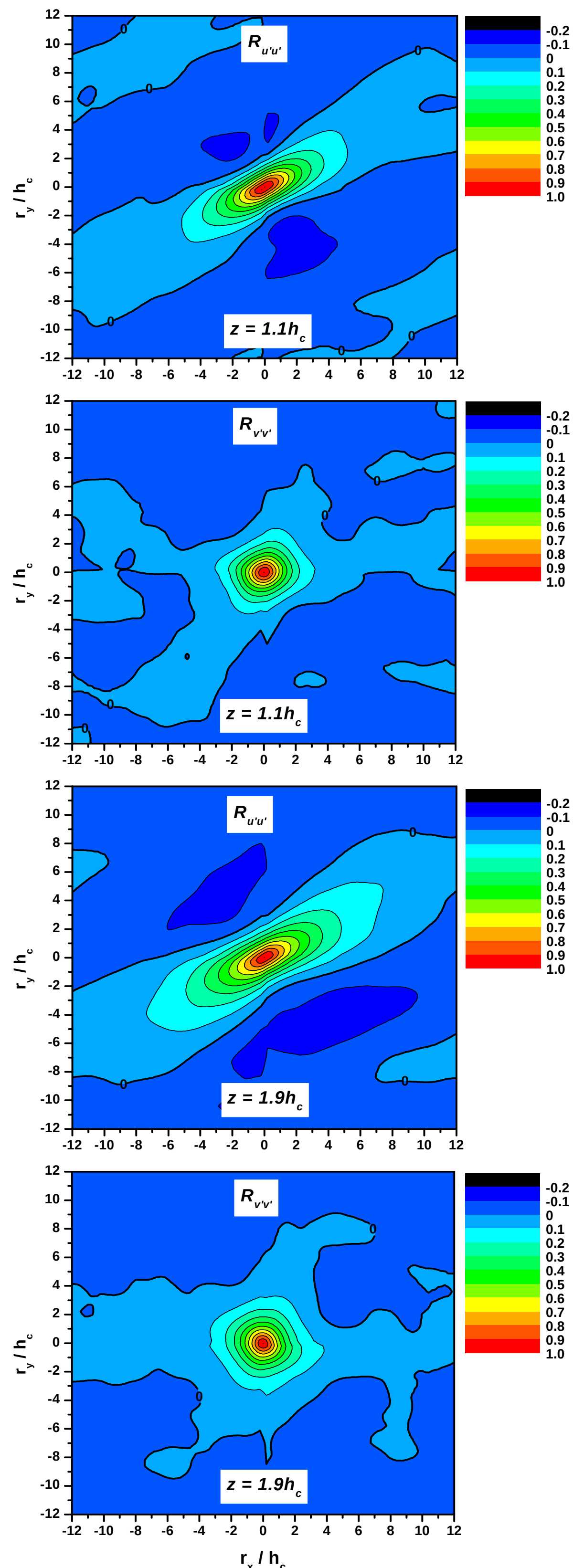

Fig. 14 Similar to Fig. 13 except that *u'* and *v'* are in a coordinate with the streamwise direction along the mean Reynolds stress direction at each height.

4. SUMMARY

A large-eddy simulation of an Ekman boundary layer with the lowest 20 m occupied by a model forest is performed. The simulation has a domain size much greater than most previous LES of canopy airflows, especially in the vertical direction. Single-point integral turbulent statistics illustrate that the depth of the roughness sublayer is about twice the canopy height. Above the roughness layer, a thin logarithmic layer appears to exist between 2.5-3 times canopy height. Two-point correlations indicate that the vertical extent of coherent structure centered near the canopy top is up to about 2-3 times the canopy height depending on whether a contour level of 0.2 or 0.1 is used (except for the two-point correlations of pressure perturbations). This is not significantly different from previous LES of canopy flow in neutral conditions. However, the horizontal extent of the coherent structures shown in the two-point correlations is appreciably greater than those in previous LES of canopy flows with smaller domain size. The effects of more extended horizontal domain, boundary layer depth and stability and canopy morphology on the roughness sublayer are still on-going investigation.

Acknowledgement: The first author would like to acknowledge support of this work from a creativity research award by the Thomas Harriot College of Arts and Sciences at East Carolina University.

References

Albertson, J.D., Katul, G.G., Wiberg, P., 2001: *Adv. Water Resour*. **24**, 1103.
Andrén, A., Moeng, C.-H., 1993: *J. Atmos. Sci.* **50**, 3366.
Dwyer, M.J., Patton, E.G., Shaw, R.H., 1997: *Boundary-Layer Meteorol*. **84**, 23.
Fitzmaurice, L., Shaw, R.H., Paw U, K.T., Patton, E.G., 2004: *Boundary-Layer Meteorol*. **112**, 107.
Kanda, M., Hino, M., 1994: *Boundary-Layer Meteorol.* **68**, 237.
Lin, C.-L., McWilliams, J.C., Moeng, C.-H., Sullivan, P.P., 1996: *Phys. Fluids.* **8**, 2626.
Lin, C.-L., Moeng, C.-H., Sullivan, P.P., McWilliams, J.C., 1997: *Phys. Fluids.* **9**, 3235.
Moeng, C.-H., 1984: *J. Atmos. Sci.* **41**, 2052.
Moeng, C.-H., Wyngaard, J.C., 1988: *J. Atmos. Sci.* **45**, 3573.
Moeng, C.-H., Sullivan, P.P., 1994: *J. Atmos. Sci.* **51**, 999.
Patton, E.G., Davis, K.J., Barth, M.C., Sullivan, P.P., 2001: *Boundary-Layer Meteorol*. **100**, 91.
Patton, E.G., Sullivan, P.P., Davis, K.J., 2003: *Quart. J. Roy. Meteorol. Soc*. **129**, 1415.
Shen, S., Leclerc, M.Y., 1997: *Agric. For. Meteorol.* **87**, 3-25.
Shaw, R.H., Schumann, U., 1992: *Boundary-Layer Meteorol.* **61**, 47.
Shaw, R.H., Patton, E.G., 2003: *Agric. For. Meteorol.* **115**, 5.
Su, H.-B., Shaw, R.H., Paw U, K.T., Moeng, C.-H., Sullivan, P.P., 1998: *Bound.-Layer Meteorol.* **88**, 363.
Su, H.-B., Shaw, R.H., Paw U, K.T., 2000: *Bound.-Layer Meteorol.* **94**, 423.
Watanabe, T., 2004: *Boundary-Layer Meteorol*. **112**, 307.
Zeman, O., 1981: *Ann. Rev. Fluid Mech.* **13**, 253.